Transient neural network dynamics in cognitive ageing

*Roni Tibon[1], Kamen A. Tsvetanov[2,3], Darren Price[1], David Nesbitt[1], Cam-CAN[4], & Richard Henson[1,5]

[1] MRC Cognition & Brain Sciences Unit, University of Cambridge, Cambridge, UK

[2] Department of Clinical Neurosciences, University of Cambridge, Cambridge, UK

[3] Department of Psychology, University of Cambridge, Cambridge, UK

[4] Cambridge Centre for Ageing and Neuroscience (Cam-CAN), University of Cambridge and MRC Cognition and Brain Sciences Unit, Cambridge, UK

[5] Department of Psychiatry, University of Cambridge, Cambridge, UK

*Corresponding author:

Dr. Roni Tibon
MRC Cognition & Brain Sciences Unit
University of Cambridge
15 Chaucer Road
Cambridge, CB2 7EF
UNITED KINGDOM
Telephone: +44 1223 355 294
Email: roni.tibon@mrc-cbu.cam.ac.uk

RUNNING TITLE: NETWORK DYNAMICS IN COGNITIVE AGEING

Pages: 35 **Tables**: 3 **Figures**: 4

Keywords: magnetoencephalography; hidden Markov model; canonical correlation analysis; ageing; cognition; fluid intelligence

Abstract

It is important to maintain cognitive function in old age, yet the neural substrates that support successful cognitive ageing remain unclear. One factor that might be crucial, but has been overlooked due to limitations of previous data and methods, is the ability of brain networks to flexibly reorganize and coordinate over a millisecond time-scale. Magnetoencephalography (MEG) provides such temporal resolution, and can be combined with Hidden Markov Models (HMMs) to characterise transient neural states. We applied HMMs to resting-state MEG data from a large cohort (N=595) of population-based adults (aged 18-88), who also completed a range of cognitive tasks. Using multivariate analysis of neural and cognitive profiles, we found that decreased occurrence of "lower-order" brain networks, coupled with increased occurrence of "higher-order" networks, was associated with both increasing age and decreased fluid intelligence. These results favour theories of age-related reductions in neural efficiency over current theories of age-related functional compensation, and suggest that this shift might reflect a stable property of the ageing brain.

1 Introduction

With the increasing proportion of older adults in the worldwide population (Beard et al., 2016), there is a pressing need to understand the neurobiology of cognitive ageing. Normal ageing generally results in cognitive decline (Hedden & Gabrieli, 2004), though not all cognitive functions follow the same trajectory. In particular, whereas age is related to a marked reduction in fluid intelligence (the ability to solve new problems), it has a much more modest effect on crystallised intelligence (the ability to rely on acquired knowledge; e.g., Borgeest et al., 2018; Gottfredson & Deary, 2004; Schaie, 1994; Tucker-Drob, 2011). Indeed, crystallised intelligence tends to increase with age, as individuals accrue knowledge across their lifespan (e.g., Ackerman & Rolfhus, 1999; Horn & Cattell, 1967; Kemper & Sumner, 2001; Uttl, 2002; Verhaeghen, 2003), although it may decline in very late decades (Bates et al., 2018; Drag & Bieliauskas, 2010; Singer et al., 2003). Moreover, functional neuroimaging has revealed that ageing is associated with different patterns of connectivity between brain regions, both within and between large-scale networks (Geerligs et al., 2014). One factor that might play a crucial role in the ability to maintain cognition in old age, but which has been largely overlooked, is the ability of brain networks to flexibly reorganise and coordinate on a sub-second time-scale. Indeed, the relationship between cognition and such transient brain connectivity, and how this relationship differs with age, remains unknown.

In recent decades, functional connectivity within the human brain has been measured mainly with functional magnetic resonance imaging (fMRI). In particular, differences in the brain's connectivity during the resting-state (rsfMRI) have proved effective in distinguishing various patient groups from controls (e.g., Alzheimer disease, major depression, schizophrenia; see for example Lee et al., 2013). Substantial work has also used rsfMRI to examine the effects of age on functional connectivity (e.g., Andrews-Hanna et al., 2007; Chan et al., 2014; Ferreira & Busatto, 2013; Geerligs et al., 2015; Grady et al., 2016; Grady, 2008). Following the suggestion that fluctuations in activity and connectivity can support flexible reorganization and coordination of neural networks (e.g., Allen et al., 2014), this notion was recently extended to the investigation of *dynamic* functional connectivity. For

example, Cabral et al. (2017) were able to link the switching dynamics of rsfMRI to cognitive performance in older age. Furthermore, Petrican and Grady (2017, 2019) showed that age moderates the relation between inhibition and dynamic organization of resting-state networks. However, interpreting connectivity differences that are measured with fMRI is difficult owing to methodological issues, such as confounding factors like vascular reactivity and head motion, which also change with age (Geerligs et al., 2017; Lehmann et al., 2017; Power et al., 2012; Tsvetanov et al., 2015). While some of these confounds, like neurovascular coupling, can be addressed by more sophisticated modelling (Tsvetanov et al., 2019), others like head-motion are notoriously difficult to correct (e.g., Maknojia et al., 2019). Furthermore, the fact remains that fMRI has a fundamentally limited temporal resolution (owing to the sluggish vascular response and relatively slow image acquisition times), which precludes it from disclosing the potentially richer dynamics in brain connectivity above approximately 0.1 Hz.

An alternative, non-invasive way of measuring functional connectivity is offered by magnetoencephalography (MEG), which can sample neural activity at 1kHz and higher (at the cost of worse spatial resolution). Indeed, recent advances in analytical approaches offer the ability to measure dynamic functional connectivity in terms of "microstates" of stable connectivity patterns that last a few hundred milliseconds (Baker et al., 2014), well beyond the temporal resolution of fMRI. Moreover, MEG is less sensitive than fMRI to age-related changes in vascular factors (Tsvetanov et al., 2015), and allows simpler and more robust methods for correcting head-motion artifacts (e.g., Taulu & Simola, 2006). In the current study, we utilized these advantages of MEG to relate transient resting-state dynamics to cognitive ageing.

More specifically, we exploited a large resting-state MEG (rsMEG) dataset obtained from 595, population-based individuals, who were sampled uniformly across the adult-lifespan (18 to 88 years of age) as part of the Cam-CAN project (www.cam-can.org). In addition to the rsMEG scan, these individuals also completed a wide range of cognitive tasks. We characterised transient network dynamics using Hidden Markov Models (HMMs) in order to explore the temporal dynamics of rsMEG

networks (Baker et al., 2014; Brookes et al., 2018; Hawkins et al., 2020; Vidaurre et al., 2016, 2017, 2018). HMM is a data-driven method that identifies a sequence of "states", where each state corresponds to a unique pattern of brain covariance that reoccurs at different points in time. By quantifying the time-series of MEG data as a sequence of transient states, the HMM provides information about the periods of time at which each state is active, enabling the characterisation of its temporal dynamics. While this technique has identified network dynamics in small resting-state or task MEG datasets (Baker et al., 2014; Hawkins et al., 2020; Vidaurre et al., 2016), these dynamics have not yet been linked to age and cognition. In particular, the size of the Cam-CAN cohort allowed us to take a multivariate approach, namely to use canonical correlation analysis (CCA) to relate the temporal properties of the data-driven HMM states to profiles of cognitive performance, and to test whether these relations differ with age.

2 Materials and Methods

2.1 Participants

A population-based sample of 708 healthy human adults (359 women and 349 men) was recruited as part of Stage 2 of the Cambridge Centre Aging and Neuroscience (Cam-CAN; www.cam-can.org; Shafto et al., 2014). Ethical approval for the study was obtained from the Cambridgeshire 2 (now East of England-Cambridge Central Research Ethics Committee), and participants gave full informed consent. Exclusion criteria included poor vision (below 20/50 on Snellen test; (Snellen, 1862) and poor hearing (threshold 35 dB at 1000 Hz in both ears), ongoing or serious past drug abuse as assessed by the Drug Abuse Screening Test (DAST-20; Skinner, 1982), significant psychiatric disorder (e.g., schizophrenia, bipolar disorder, personality disorder), neurological disease (e.g., known stroke, epilepsy, traumatic brain injury), low score in the Mini Mental State Exam (MMSE; 24 or lower; Folstein et al., 1975), or poor English knowledge (non-native or non-bilingual English speakers); a detailed description of exclusion criteria can be found in Shafto et al. (2014), Table 1. Of these, only participants with full neuroimaging data (resting state MEG data and structural MRI data) were considered for the

current study (*n* = 610). Fifteen additional participants were excluded from analyses due to poor MEG-MRI co-registration (details below). Thus, the final sample included 595 participants (299 women and 296 men, age range 18-88).

2.2 Cognitive Tasks

Thirteen cognitive tasks, performed outside the scanner, were used to assess five broad cognitive domains, including executive function, memory, language, processing speed and emotional processing. The tasks are summarized in Table 1, with full detail in Shafto et al. (2014). Task scores were obtained from Borgeest et al. (2018), in which missing data (<12% in all tasks) were interpolated using Full Information Maximum Likelihood (Enders & Bandalos, 2001) across the full Stage 2 sample (*n* = 708), as implemented in the Lavaan R package (Rosseel, 2012).

Table 1. Description of cognitive behavioural tasks (table adapted from Borgeest et al., 2018)

Cognitive Domain	**Cognitive Task**	**Task Description**	**Descriptive Statistics for *n*=595 (Mean, SD, Range)**	**References**
Executive Function	Fluid Intelligence (FldIn)	Cattell Culture Fair Test: nonverbal puzzles involving series completion, classification, matrices, and conditions.	*M* = 31.74 *SD* = 6.83 *Range* = 11-44	Cattell & Cattell, 1960
	Multitasking (Hotel Task; MltTs)	Simulated tasks of a hotel manager: write customer bills, sort money, proofread advert, sort playing cards, alphabetise list of names. Total time must be allocated equally between tasks; there is not enough time to complete any one task.	*M* = 301.3 *SD* = 171.7 *Range* = 20.19-960	Shallice & Burgess, 1991
Language Functions	Spot the Word (StW)	Pairs of items comprising one word and one non-word (e.g, 'flonty – xylophone'); participant is required to point to the real word.	*M* = 53.72 *SD* = 5.28 *Range* = 24-60	Baddeley, Emslie & Nimmo-Smith, 1993
	Sentence Comprehension (SntRec)	Judge grammatical acceptability of partial auditory sentences, which begin with an ambiguous sentence stem (e.g., "Tom noticed that landing planes…") followed by a disambiguating continuation word (e.g., "are") in a different voice. Ambiguity is either semantic or syntactic, with empirically determined dominant and subordinate interpretations.	*M* = 0.89 *SD* = 0.07 *Range* = 0.46-1	Rodd, Longe, Randall, & Tyler, 2010
	Picture-Picture Priming (PicNam)	Name the pictured object presented alone (baseline), then when preceded by a prime object that is phonologically related (one, two initial phonemes), semantically	*M* = 0.78 *SD* = 0.09 *Range* = 0.5-0.94	Clarke, Taylor, Devereux, Randall, & Tyler, 2013

		related (low, high relatedness), or unrelated.		
	Verbal Fluency (VrbFl)	Mean of letter (phonemic) fluency and animal (semantic) fluency task. For phonemic fluency task, participants have 1 min to generate as many words as possible beginning with the letter 'p'. For semantic fluency task, participants have 1 min to generate as many words as possible in the category 'animals'.	*M* = 20.72 *SD* = 5.4 *Range* = 6-37.5	Lezak, Muriel, & Deutsch, 1995
	Proverb Comprehension (ProV)	Read and interpret three English proverbs.	*M* = 4.54 *SD* = 1.62 *Range* = 0-6	Hodges, 1994
Emotional Processing	Face Recognition (FaceRec)	Given a target image of a face, identify same individual in an array of 6 face images (with possible changes in head orientation and lighting between target and same face in the test array)	*M* = 22.93 *SD* = 2.32 *Range* = 14-27	Benton, 1994
	Emotion Expression Recognition (EmoRec)	View face and label emotion expressed (happy, sad, anger, fear, disgust, surprise) where faces are morphs along axes between emotional expressions.	*M* = 86.6 *SD* = 10.74 *Range* = 47.5-100	Ekman & Friesen, 1976
Memory	Visual Short-Term Memory (VSTM)	View (1–4) coloured discs briefly presented on a computer screen, then after a delay, attempt to remember the colour of the disc that was at a cued location.	*M* = 2.43 *SD* = 0.58 *Range* = 0*-3.5	Zhang & Luck, 2008
	Story Recall (StrRec)	Listen to a short story, recall freely immediately after, then again after a delay, and finally answer recognition memory questions. Delayed recall measure used here.	*M* = 12.98 *SD* = 4.23 *Range* = 0*-24	Wechsler, 1999
Processing Speed	Choice Motor Speed (MRSp)	Time-pressured movement of a cursor to a target by moving an (occluded) stylus under veridical, perturbed (30°), and reset (veridical again) mappings between visual and real space.	*M* = 0.19 *SD* = 0.06 *Range* = 0.05-0.85	
	Choice Motor Coefficient of Variation (MRCv)	Standard deviation divided by mean of reaction time of choice motor speed. Reflects the relative measure of variability.	*M* = 1.84 *SD* = 0.38 *Range* = 0.91-2.98	

Note: reanalysis of the data after excluding one participant who scored 0 in the StrRec measure, and another who scored 0 in the VSTM measure, resulted in the exact same patterns.

2.3 MEG data acquisition and pre-processing

Figure 1 shows an overview of the preprocessing and analysis pipeline for the study. Data were collected using a 306-channel VectorView MEG system (Elekta Neuromag, Helsinki), consisting of 102 magnetometers and 204 orthogonal planar gradiometers, located in a magnetically shielded room. MEG resting state data (sampled at 1 kHz with a highpass filter of 0.03 Hz) were recorded for 8 min and 40 s, while participants remained still in a seated position with their eyes closed, but instructed

to stay awake. Head position within the MEG helmet was estimated continuously using four Head-Position Indicator (HPI) coils to allow offline correction of head motion.

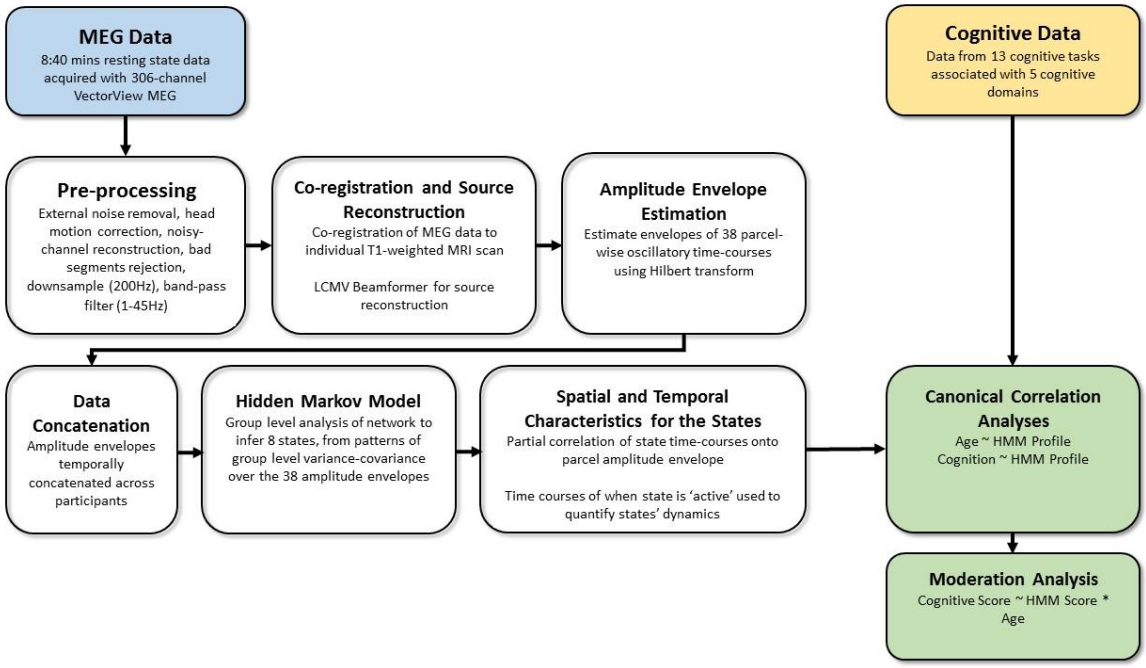

Figure 1. Overview of processing and analysis pipeline used in the study.

The MaxFilter 2.2.12 software (Elekta Neuromag Oy, Helsinki, Finland) was used to apply temporal signal space separation (tSSS, Taulu & Simola, 2006) to the continuous MEG data to remove noise from external sources (correlation threshold 0.98, 10-sec sliding window), to continuously correct for head-motion (in 200-ms time windows), to remove mains-frequency noise (50-Hz notch filter), and to detect and reconstruct noisy channels. Following these de-noising steps, data were imported into Matlab (The MathWorks, Inc.) and preprocessed using a mixture of SPM12 (http://www.fil.ion.ucl.ac.uk/spm) and the OHBA Software Library (OSL; https://ohba-analysis.github.io/osl-docs/). Bad segments were detected and rejected by identifying outliers in the standard deviation of the signal using the Generalized ESD test (Rosner, 1983) at a significance level of a 0.1 (mean % segments rejected = 1.44, *SD* = 1.35). Data were then down-sampled to 200Hz, and a band pass filter was applied from 1–45 Hz to remove slow trends and high frequency noise.

2.4 MEG source reconstruction, parcellation, and envelope calculation

The MEG data were co-registered to each participant's structural T1-weighted MRI, using three anatomical fiducial points (nasion, and left and right pre-auricular points) that were digitized for the MEG data and identified manually on the MRIs. The median distance between each scalp headshape point and its nearest vertex was calculated for each participant, and those with a median distance greater than 6 mm (*n*=15; see *Participants* section above) were excluded from subsequent analyses.

Source space activity was then estimated for each participant at every point of an 8 mm whole-brain grid using a single-shell lead-field model and a linearly constrained minimum variance (LCMV) scalar beamformer (Van Veen et al., 1997; Woolrich et al., 2011), combining data from both magnetometers and gradiometers. Source-reconstructed time-series (in each epoch) for each grid point were then parcelled into 38 regions of interest (ROIs; defined by selecting a subset of 19 of the ROIs in the Harvard–Oxford cortical brain atlas, available in FSL, and splitting each into two lateral halves to create 38 binary ROIs, as in Colclough et al. (2015). This was done in order to reduce the dimensionality of the oscillatory activity submitted to the HMM (see below). The reconstructed data for each parcel was summarised by the first principal component across grid points within that parcel, and magnetic field spread between parcels was reduced by symmetric, multivariate orthogonalization (Colclough et al., 2015; Colclough et al., 2017). Next, the amplitude envelope of each parcel's time-course was calculated using a Hilbert transform, subsequently down-sampled to 20 Hz for computational efficiency.

2.5 Group level exploratory analysis of networks (Hidden Markov Model)

We used the group-level exploratory analysis of networks (GLEAN) toolbox (https://github.com/OHBA-analysis/GLEAN; Vidaurre et al., 2017), which assumes that the same set of microstates apply to all participants. The de-meaned and normalized envelope data for each participant were concatenated temporally across all participants to produce a single dataset. We set

the analysis a-priori to derive 8 states from the data, based on a previous work (Baker et al., 2014) that used the same HMM approach to examine transient dynamics of rsMEG networks. In that study, the authors gradually increased the number of inferred states from 4 to 14. Increasing the number of states did not change their topographies, nor revealed any additional distinct topographies, but rather resulted in the splitting of states into multiple similar maps. The authors concluded that there is no advantage of using more than 8 states when aiming to identify resting-state networks, and that this number represents a reasonable trade-off between a sufficiently rich but not overly complex representation (Baker et al., 2014).

HMMs describe the dynamics of brain activity as a sequence of transient events, each of which corresponds to a visit to a particular brain state. Each state describes the data as coming from a unique 38-dimensional multivariate normal distribution, defined by a covariance matrix and a mean vector. Therefore, each state corresponds to a unique pattern of amplitude envelope variance and covariance that reoccurs at different time points. The HMM state time-courses then define the points in time at which each state was “active” or “visited”. These estimated state time-courses, represented by a binary sequence showing the points in time when that state was most probable, were obtained using the Viterbi algorithm (Rezek & Roberts, 2005). The partial correlation of the time-course of each state (i.e., after adjusting for the time-courses of all the other states) with the whole-brain parcel-wise amplitude envelopes concatenated across participants, were estimated in order to produce spatial maps of the changes in amplitude envelope activity associated with each state. The resulting state maps show the brain areas whose amplitude envelopes increase or decrease together (covary) when that state is active, compared to what happens on average over time.

Using the state time-courses, we quantified the temporal characteristics of each state according to four measures of interest: (1) Fractional Occupancy (FO): the proportion of time the state was active; (2) Mean Life Time (MLT): the average time spent in the state before transitioning to

another state; (3) Number of Occurrences (NO): the number of times the state was active; and (4) Mean Interval Length (MIL): the average duration between recurring visits to that state.

2.6 Relating HMM states to age and cognition (Canonical Correlation Analyses)

To identify how the temporal characteristics of the HMM states relate to age and cognition, we used Canonical Correlation Analyses (CCA; Smith et al., 2015; Sui et al., 2012; Wang et al., 2020; see Figure 1 in Wang et al. (2020) for schematic illustration of CCA). CCA is a multivariate technique that can identify and measure linear relations between two sets of variables. Linear combinations within each of the sets are defined such that the correlations of these combinations between sets (e.g., between HMM profile and cognitive profile) are maximized, resulting in CCA components, or "modes". This multivariate approach is useful when the observed variables within each set are correlated (as is the case for the above HMM temporal characteristics, and for the cognitive scores).

CCA was employed via *canoncorr* in Matlab. The number of modes produced by this analysis is always equal to the minimum number of variables across the two sets (though not all modes necessarily explain a substantial portion of the variance, see *Results* section below). Each mode represents a set of function coefficients, which are the standardized coefficients derived to maximize the canonical correlations, and are analogous to beta weights in regression. In canoncorr's terminology (see also Smith et al., 2015; Sui et al., 2012; Wang et al., 2020), each CCA mode is also associated with canonical "coefficients" across the variables in each set and "scores" across the observations (participants). The correlation between each set's participant scores (for a given mode) is termed the "canonical correlation" (denoted by R_c), and its squared value (R^2_c) represents the proportion of variance shared between the sets. The correlation between the participant scores and each original variable (for a given set and given mode) is called the "structure coefficient" (denoted by r_s), and the set of structure coefficients represents the "profile" of the CCA mode across those variables. Structure coefficients are often used to guide interpretation of multivariate analyses, and are particularly useful in the presence of multicollinearity (Sherry & Henson, 2005). In the Results

section below, structure coefficients greater than |.2| are highlighted to indicate substantial contribution of the variable to the canonical solution (see Smith et al., 2015, in which the same cut-off value was used).

All variables were z-scored before being subjected to CCA, in order to make the various parameters more comparable across variables. First, we used CCA to relate the 4 temporal characteristics across all 8 HMM states (Set 1, 32 variables) to age. Note that in this case, the CCA analysis is equivalent to multiple linear regression because the second set contains a single variable (age). Nevertheless, for consistency with subsequent analysis, we used CCA rather than multiple linear regression. We then conducted another CCA analysis to relate the 32 HMM measures (Set 1) to the 13 cognitive measures (Set 2). Having used CCA to establish relationships between the HMM brain measures and the cognitive measures across all ages, we then asked whether the relationship between HMM profile and cognitive profile (i.e., the relations between canonical scores obtained by the final CCA) varied with age, using a moderation analysis (see Tsvetanov et al., 2016, 2018), for a similar approach with different measures). Specifically, we constructed a multiple linear model where HMM scores (for a given mode), age and their interaction term (HMM scores × age) were used as independent variables and cognitive scores (for that mode) as the dependent variable (all statistical tests were two-sided). In order to visualise the results of this continuous moderation analysis, we created scatter plots of HMM profile versus cognitive profile for six equally-sized age groups (n = 99 in each group).

2.7 Additional control analyses

In addition to the main analyses described above, we performed several additional analyses in order to ensure that the CCA results are robust and interpretable. First, in order to ascertain that the results are not biased by outliers, we repeated the main CCA and moderation analyses after excluding data from participants who were outliers in one or more measures. Second, in order to check whether the results reflect variations in the HMM states' expression across participants, we correlated each

participant's state map (based on the partial correlation of their ROI data with the timeseries of the states; see earlier) with the group-averaged map for that state. Then, for each state, we correlated these correlation coefficients with age, to determine whether the states were similarity expressed across age. The significance of this correlation was estimated against a distribution of 10,000 correlation coefficients based on permuting participants' ages. Third, in order to confirm the significance of canonical correlation (R_c) of the first CCA mode that was determined under parametric assumptions, we also estimated R_c against a distribution of 10,000 correlation coefficients based on a CCA computed after permuting across participants their cognitive scores. Fourth, we performed a separate cross-validation analysis in which the CCA was only run on a subset of the data, and the outputs tested against the rest. This analysis was performed over 10,000 iterations. For each iteration, we randomly chose 80% of the participants for the "training" subset, leaving the other 20% for the "testing" subset, and computed the R_c for the first CCA mode in the testing subset, using the weights from the training set. Fifth, in order to assure that the function weights are stable, we implemented split-half reliability testing (e.g., Kovacevic et al., 2013), by splitting the sample into two equal-sized subsets, running the CCA analysis separately for each subset, and computing the correlation between the 45 standardized canonical function coefficients (32 coefficients for the HMM brain measures + 13 coefficients for the cognitive measures) obtained from the two subsets. We repeated this process over 10,000 iterations, randomly splitting the participants into the two subsets in each iteration. Finally, we repeated the HMM-age CCA analysis with an additional quadratic term, in order to account for potential non-linear (quadratic) age-effects. Moreover, in addition to these control analyses, we computed a transition probability and used CCA to relate these transitions to age. Further details of this analysis and the results are reported in Supplementary Analysis 1 and Supplementary Figure 6.

2.8 Data and code availability

Raw data from the Cam-CAN project are available from http://camcan-archive.mrc-cbu.cam.ac.uk, subject to conditions specified on that website. For a complete description of Cam-

CAN data and pipelines, see Shafto et al. (2014) and Taylor et al. (2017). In addition, pre-processed mean data used for analyses and figures, together with all the analysis code, is available on: https://osf.io/7d4wj/?view_only=ccc8d930e0aa4b99a93734b8fb76af9e.

3 Results

3.1 Global spatial and temporal characteristics of HMM states

Figure 2 shows the spatial maps of the 8 networks (states) derived from combining the MEG data across all participants. The states include three distributed frontotemporoparietal networks (FTP1, FTP2, FTP3), a higher-order visual network (HOV), two early visual networks (EV1, EV2) and two sensorimotor networks (SM1, SM2). They are similar to those obtained from young adults in previous studies (Baker et al., 2014; Brookes et al., 2018; Hawkins et al., 2020). Note that these spatial maps represent increases (warm colours) or decreases (cool colours) in power compared to mean power across the time-course. Nevertheless, they do not capture all that drives the state divisions, as there is also the state covariance matrix that captures functional connectivity differences. Thus even though the spatial distribution of power in EV1 may look like the inverse of that in EV2 (and likewise for SM1 and SM2), these states still differ in the functional connectivity between ROIs.

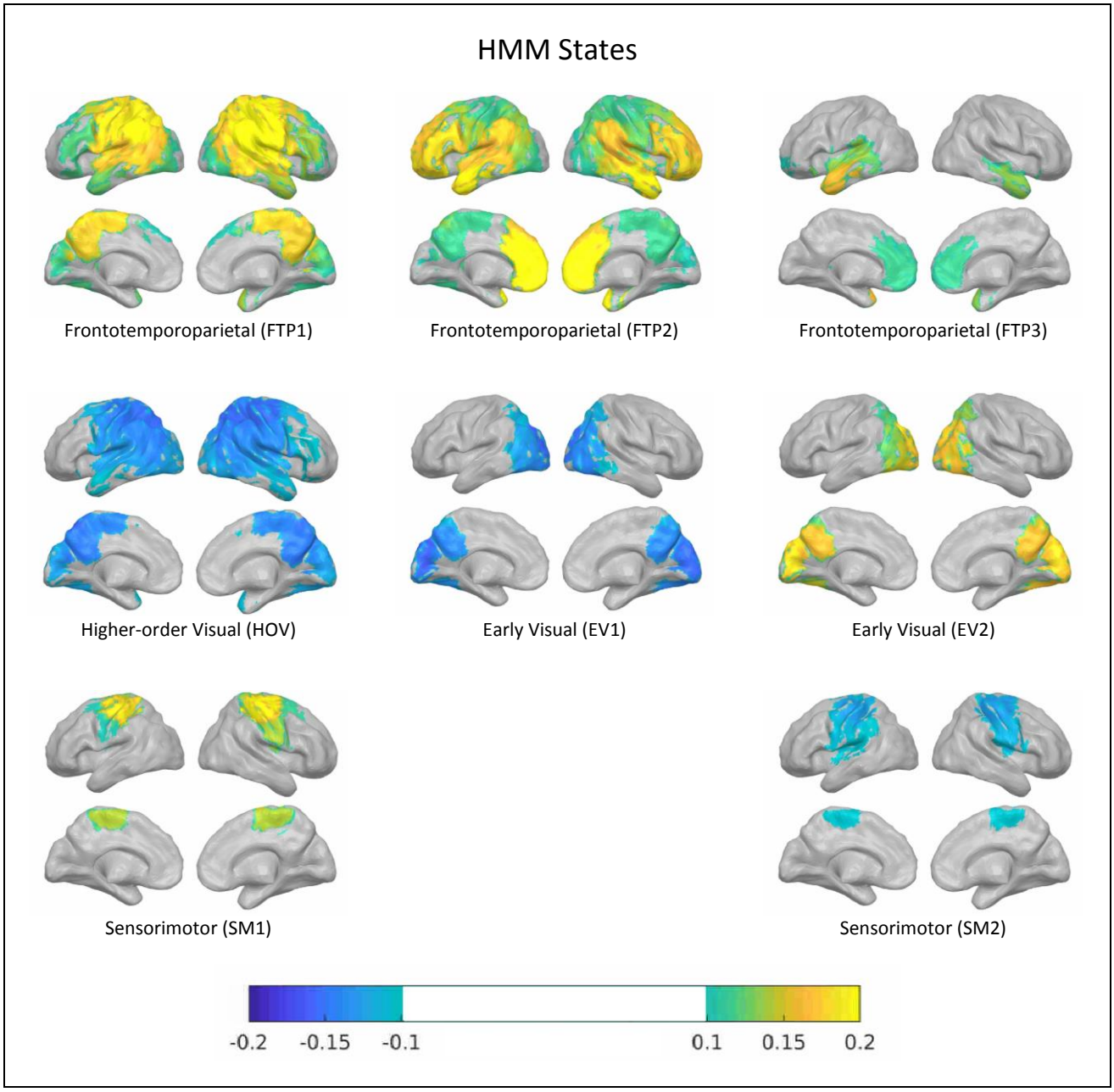

Figure 2. The 8 inferred HMM states. Each map shows the partial correlation between the state time course and the parcel-wise amplitude envelopes. Yellow colours represent amplitude envelope increases when the brain visits that state and blue colours represent envelope decreases. The partial correlation values have been thresholded to show correlation values above 50% of the maximum correlation across all states. To refer to the states, we use the same naming scheme applied by Hawkins et al. (Hawkins et al., 2020).

We next characterised the temporal properties of each state in terms of 4 metrics: fractional occupancy (FO), mean life time (MLT), number of occurrences (NO) and mean interval length (MIL). Group averages for each measure in each state are shown in Figure 3. Overall, primary (visuo-motor) states had higher number of occurrences than higher-order states. The most commonly-occurring networks were sensorimotor network SM2 and early visual network EV1, which had the highest mean FO and NO. The network with the most prolonged visits (highest MLT) was the high-order visual network HOV. Conversely, the least common network, with lowest FO and NO but greatest MIL, was frontotemporoparietal network FTP3. These findings largely agree with Hawkins et al. (2020) and (to a lesser extent) with other previous studies (Baker et al., 2014; Brookes et al., 2018), though now based on a much larger sample with a much larger age range.

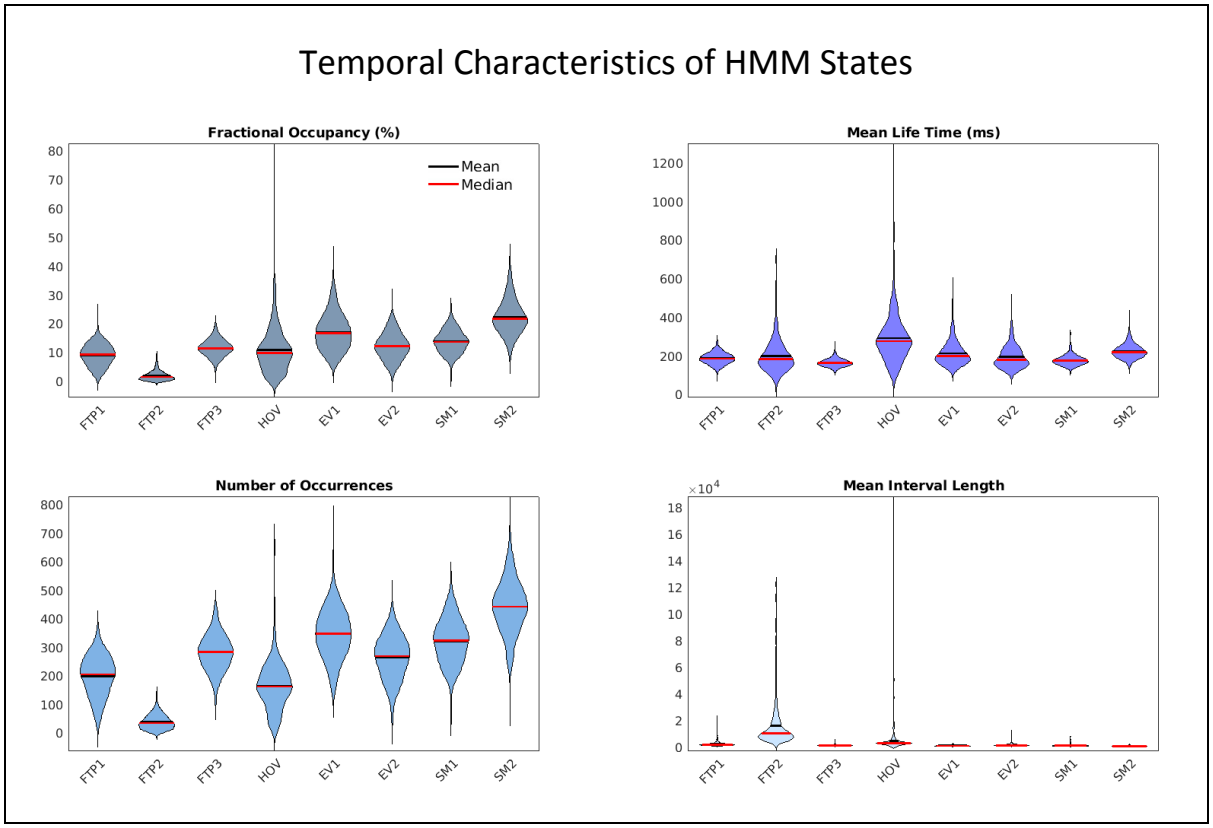

Figure 3. Violin plots (Hoffmann, 2015) of the four temporal characteristics of the HMM states: % fractional occupancy (FO; top-left), mean life time (MLT; top right), number of occurrences (NO; bottom-left) mean interval length (MIL; bottom-right). The first three measures are positive measures (i.e., indicate more frequent/longer duration of state's occurrence), whereas the fourth measure (MIL) is a negative measure. The various states are indicated as *FTP* (frontotemporoparietal), *HOV* (higher-order visual), *EV* (early-visual) and *SM* (sensorimotor). Mean and median are indicated by black and red lines, respectively (N=595). See also Supplementary Figure 2, for violin plots of the temporal characteristics following the removal of outliers: the pattern of results remained unchanged, but the skewness (e.g., for HOV) was moderated.

3.2 HMM states are related to both age and cognition

Our next step was to apply CCA to relate the 32 temporal characteristics of the HMM states (4 metrics for each of the 8 states) to age. One participant who had no visits to one of the states (HOV) was excluded from this analysis. Only a single CCA mode was possible (given the unidimensional age variable), which explained 28.6% of the combined variance (R_c = .53, p < .001). Table 2 shows the structure coefficients (r_s) for each metric of each state. As apparent in Table 2, the three frontotemporoparietal states (FTP1, FTP2, FTP3), the higher-order visual state (HOV), and one of the sensorimotor states (SM1) tended to show positive correlations with age for FO, MLT and NO measures, and negative correlation for the MIL measure, whereas the two early visual states (EV1 and EV2) tended to show negative correlations with age for FO, MLT, NO and positive correlation for MIL. In other words, older people had more and longer occurrences of states involving frontotemporoparietal, higher-order visual, and sensorimotor states (with the exception of sensorimotor state SM2, which did not show strong relationship with age), and fewer, shorter occurrences of early visual states.

Table 2. Structure coefficients for the CCA relating HMM measures with age (N=594)

State	Fractional Occupancy	Mean Lifetime	Number of Occurrences	Mean Interval Length	Age
FTP1	.27	.13	.28	-.12	(1)
FTP2	.23	.15	.24	-.21	
FTP3	.20	.44	.12	-.07	
HOV	.23	.15	.34	-.07	
EV1	-.35	-.50	-.00	-.01	
EV2	-.45	-.38	-.33	.18	
SM1	.18	.04	.22	-.13	
SM2	-.03	-.09	.00	.02	

**p<.05, **p<.005.* Note: Each cell depicts structure coefficients (r_s). Structure coefficients greater than |.2| are underlined. Coefficients are shown for each of the 4 HMM measures, for each state. The various states are indicated as *FTP* (frontotemporoparietal), *HOV* (higher-order visual), *EV* (early-visual) and *SM* (sensorimotor). r_s for Age is 1, because this set contains only one variable. See also Supplementary Table 1 for the function coefficients.

Once we established the effects of age on the pattern of occurrence of brain states, we asked how this pattern of occurrence relates to cognition. To this end, we related the temporal characteristics of the states to the 13 cognitive measures (see Methods). Twelve CCA modes showed a significant correlation coefficient (Bonferroni corrected p-value across 13 modes < .05).

Nevertheless, given the relatively low squared canonical correlation (R^2_c) of most modes (see Supplementary Figure 1), only the first mode, which accounted for 24% of the combined variance, was explored further (see Sherry & Henson, 2005 for a similar approach). Figure 4 presents the structure coefficients (r_s) of the first CCA mode (Supplementary Table 2 further shows the function coefficients). For the cognitive data, the coefficients resembled the pattern associated with poor (low) fluid intelligence that has been reported before (Borgeest et al., 2018). Specifically, r_s was appreciably different from zero for all the tests except the proverbs (ProV) and Spot-the-Word (STW) tests, which capture instead crystallised intelligence. Furthermore, it was negative for all fluid intelligence tasks, except multitasking (MltTs) and motor speed (MRSp) tests, where a positive r_s value also means worse fluid intelligence, because longer response-time measures represent worse performance. Importantly, the four "higher-order" states (FTPs and HOV) were positively related to this cognitive profile, i.e., greater occurrence of these states (as indicated by increased FO, MLT, NO and decreased MIL) was associated with lower fluid intelligence. Furthermore, this cognitive profile was associated with decreased activation of the two early visual states (EVs). The two sensorimotor states did not show strong relations to this cognitive profile.

3.3 Age moderates the relation between HMM states and cognition

Finally, we asked whether the relationship between the HMM brain profile and the cognitive profile differed with age. For this moderation analysis, we constructed a multiple linear regression model that included participants' scores for the HMM profile, their age and the interaction (HMM profile × age) as predictors, and participants' scores for the cognitive profile as the dependent variable. The HMM scores were significantly associated with cognitive scores after accounting for the main effect of age (β = .13, $t(590)$ = 4.51, $p < .001$), demonstrating that the above brain-cognitive relationship was not driven solely by age effects. Moreover, the interaction between age and HMM profile was also significant (β = .11, $t(590)$ = 4.33, $p < .001$), demonstrating that the brain-cognition relationship was moderated by age in a positive sense, i.e., becoming more positive with age. To

visualise this moderation effect, the brain-cognition relation was repeated for six equally-sized age groups (n=99 for each group; 18–34 years old; 34-45 years old; 45-55 years old; 55-66 years old; 66-76 years old; 76-88 years old). As shown in Figure 4, the brain-cognition relationship was stronger in the older groups.

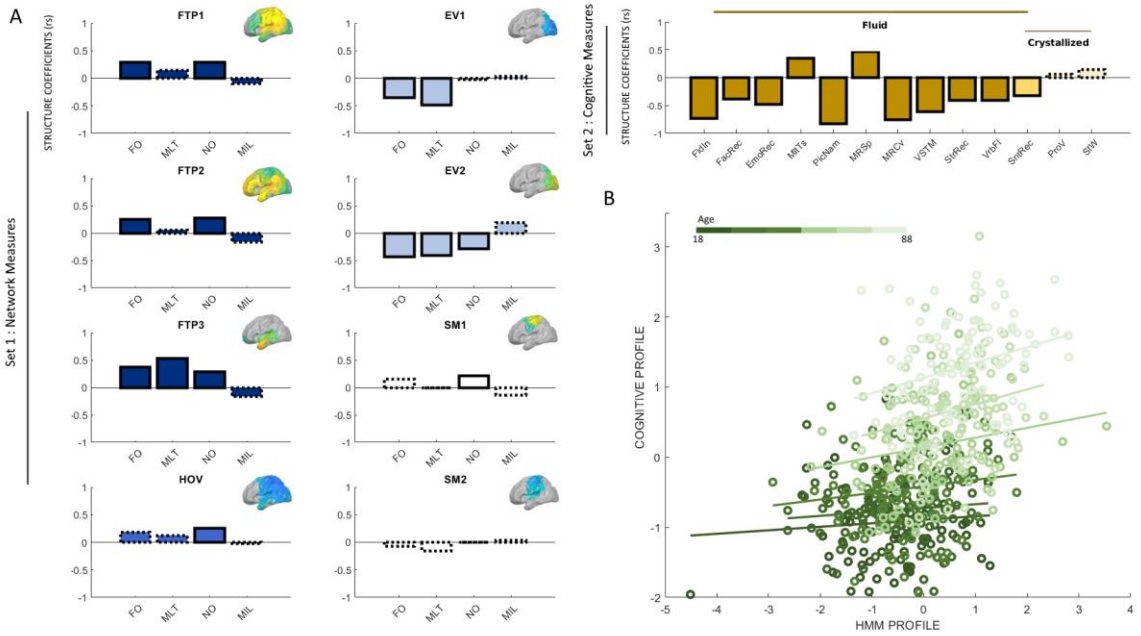

Figure 4. Outcomes of main CCA and moderation analyses (N=594). **(A)** Structure coefficients (r_s) for the CCA relating HMM measures with cognitive measures. Solid outlines represent structure coefficients greater than |.2|, whereas dashed outlines represent structure coefficients smaller than |.2|. r_s for brain HMM measures are shown in blue/white, with different shades of blue representing different types of states. HMM measures are indicated as *FO* (fractional occupancy, *MLT* (mean lifetime), *NO* (number of occurrences), and *MIL* (mean interval length). The various states are indicated as *FTP* (frontotemporoparietal), *HOV* (higher-order visual), *EV* (early-visual) and *SM* (sensorimotor). Corresponding HMM state maps are inset. For clarity, r_s for each network are shown separately, though in practice all were included in a single CCA analysis. r_s for the cognitive measures are shown in brown. Cognitive measures are fluid intelligence (*FldIn*), face recognition (*FacRec*), emotional expression recognition (*EmoRec*), multitasking (hotel task; *MltTs*), picture-picture priming (*PicNam*), choice motor speed (*MRSp*), choice motor coefficient of variation (*MRCv*), visual short-term memory (*VSTM*), story recall (*StrRec*), verbal fluency (*VrbFl*), sentence comprehension (*SntRec*), proverb comprehension (*ProV*), and spot the word (*StW*). Different shades indicate the distinction between cognitive abilities obtained via confirmatory factor analysis in Borgeest et al. (Borgeest et al., 2018): fluid intelligence (dark brown), crystallised intelligence (light brown) or both (intermediate brown; for SntRec). For the response-time measures of MltTs and MPSp, lower scores indicate better performance (hence the opposite sign). **(B)** Scatter plot of bivariate correlations for six age groups. Dark shades of green represent younger adults, whereas light shades represent older adults. The relationship between HMM and cognitive profiles is higher for older adults (formally confirmed by a continuous moderation analysis; see text).

3.4 Additional control analyses

As described above, we performed several additional analyses in order to ensure that the results are robust and interpretable. First, some of the temporal measures of the HMM states (and

MIL in particular) included a relatively large number of outliers (see Figure 3). Therefore, we repeated the main CCA and moderation analyses after excluding 98 participants depicting outliers (*SD*>3, n=496) in one or more measures. Following this removal, the temporal characteristics of the HMM states remained similar to that observed with the full sample (see Supplementary Figure 2). Moreover, the first CCA mode remained highly significant (R_c = .512, R^2_c = 26%, p < .001), and the pattern of structure correlations remained remarkably similar to that observed with the full sample (see Supplementary Figure 3). The results of the moderation analysis were also similar, with a significant association between HMM and cognitive profiles after accounting for the main effect of age (β = .16, $t(492)$ = 5.18, p < .001), together with a significant interaction between age and HMM profile (β = .13, $t(492)$ = 4.84, p < .001).

Second, for the majority of states, the HMM expression did not correlate with age (see Supplementary Figure 4), suggesting that the adherence with the general pattern observed across the sample was similar across ages. Nevertheless, for three states (FTP3, EV1 and SM2), the HMM expression significantly correlated with age, which we consider further in the Discussion.

Moreover, we estimated R_c against a distribution of 10,000 correlation coefficients based on permuting across participants their scores for the cognitive data. The canonical coefficient for the true data (R_c = .49) was greater than that of the random permutations (equivalent to p < .01, see Supplementary Figure 5). Furthermore, our cross-validation analysis yielded canonical correlations across training sets for the first mode that were similar to the original result (ranging between .45 and .56). For each iteration, we took the CCA HMM and cognition weight vectors for the first mode from the training subset, and multiplied them by the testing subset, in order to estimate participant scores for HMM and cognition. We then computed the correlation between these scores to estimate the canonical coefficient for the testing subset. Mean R_c was .32 (mean p = .007, see Supplementary Figure 5 for the full distribution). Importantly, the canonical coefficient was significant at p < .05 for 96.7% of

the testing subsets and at p < .001 for 63.7% of the testing subsets. Taken together, the results of these analyses confirm that the first CCA mode was highly significant.

In addition, correlating the standardized canonical function coefficients to assess the stability of the function weights yielded mean absolute ρ of .32 (we use an absolute ρ because negative and positive correlations indicate the same pattern of relations across variables; mean ρ = .089, see Supplementary Figure 5 for the full distribution). The correlation was significant at $p < .001$ for 35.9% of the testing subsets and at $p < .05$ for 72.4% of the testing subsets. This suggests that the function weights were stable overall, although some degree of sample-dependent fluctuation was also observed.

Finally, to investigate potential non-linear (quadratic) age-effects, we computed a quadratic age term, orthogonal to the linear age term, and ran a CCA analysis that related the 4 HMM measures across all 8 states (Set 1, 32 variables) to both age terms (Set 2, 2 variables). Both possible CCA modes were significant ($p < .001$) and explained 28.6% and 12.3% of the shared variance, respectively. The structure coefficients (r_s) are shown in Table 3 below. The important finding is that the first CCA mode, which was dominated by the (orthogonalized) linear term, was associated with the age-related shift from lower to higher-order states that was shown above. The second component was dominated by the quadratic term instead, had different HMM temporal characteristics, and is considered further in the Discussion.

Table 3. Structure coefficients for the CCA relating HMM measures with linear and quadratic age (N=594)

CCA Mode I						
State	Fractional Occupancy	Mean Lifetime	Number of Occurrences	Mean Interval Length	linAge	quadAge
FTP1	.27	.14	.28	-.12	.99	.02
FTP2	.23	.15	.24	-.21		
FTP3	.19	.44	.11	-.07		
HOV	.24	.16	.35	-.08		
EV1	-.35	-.51	-.00	-.01		
EV2	-.45	-.38	-.33	.18		
SM1	.18	.04	.22	-.13		
SM2	-.03	-.08	.00	.02		
CCA Mode II						
State	Fractional Occupancy	Mean Lifetime	Number of Occurrences	Mean Interval Length	linAge	quadAge
FTP1	-.04	-.35	.05	.01	-.02	.99
FTP2	.04	-.15	.10	-.05		
FTP3	.52	.25	.46	-.46		
HOV	-.42	-.50	-.31	.25		
EV1	.21	.07	.17	-.27		
EV2	.08	-.11	.19	-.19		
SM1	.10	-.32	.21	-.30		
SM2	-.04	-.27	.06	-.11		

**p<.05, **p<.005.* Note: Structure coefficients (r_s) for two CCA modes are presented. Structure coefficients greater than |.2| are underlined. Coefficients are shown for each of the 4 HMM measures, for each state. The various states are indicated as *FTP* (frontotemporoparietal), *HOV* (higher-order visual), *EV* (early-visual) and *SM* (sensorimotor).

4 Discussion

Our results show that transient neural dynamics, particularly those of high-order and early-visual states, differ across the healthy adult lifespan, with an increasing importance for cognitive function in older than younger adults. Importantly, by using a novel data-driven method to infer brain states from MEG data, we were able to overcome some of the limitations of the more common use of fMRI to examine ageing and cognition, such as confounding effects of vascular health, head motion and the ability to examine only very slow dynamics owing to low-frequency fluctuations of the fMRI response. More specifically, our finding that age and decreased fluid intelligence are associated with increased occurrence of brain states involving “higher-order” networks (such as those straddling frontal, temporal and parietal cortex) are less consistent with theories of functional compensation in ageing, and more consistent with theories of reduced neural efficiency in ageing, as we expand below.

We used a multivariate analysis (CCA) to relate the pattern of brain dynamics (HMM profile) to age and to cognition, and to examine whether the brain-cognition relationship was moderated by

age. This first analysis relating brain dynamics to age showed that the occurrence (e.g., frequency and duration) of states involving fronto-temporo-parietal and higher-order visual regions increase with age, whereas the occurrence of states involving early-visual regions decrease with age. The second analysis relating brain dynamics to cognitive performance revealed that a similar profile of increased occurrence of higher-order states and reduced occurrence of early-visual states is associated with a pattern of poorer performance on tests of fluid intelligence, but not tests of crystallised intelligence. Importantly, our final moderation analysis showed that this relationship between brain and cognitive profiles is not simply a result of shared influences of age (since age was included as a covariate). Moreover, this moderation analysis showed that the brain-cognitive relationship gets stronger with increased age, such that reduced cognitive performance in older participants is more strongly associated with the shift from early visual to higher-order networks than in younger participants.

Dynamic fMRI resting state connectivity was recently linked to overall performance in an extensive neuropsychological assessment battery (Cabral et al., 2017). In particular, better cognitive performance was associated with increased stability of resting states functional connectivity (i.e., prolonged lifetime and reduced switching between brain states). Other studies have revealed that resting state dynamics depend on age. For example, by measuring multiscale entropy (MSE) to assess the variability of EEG and MEG brain signal, McIntosh et al. (2014) were able to characterise developmental changes by decreased amount of local information processing, coupled with an increase in distributed information processing (see also Brookes et al., 2018, for age-effects on dynamic neural networks from mid-childhood to adulthood). Nevertheless, to our knowledge, this is the first study to report a resting state shift from lower to higher-order networks in adults that is linked to both age and cognition.

This finding nevertheless shares some similarity with previous fMRI findings. For example, (Davis et al., 2008) summarised a pattern across a number of fMRI experiments (first observed by Grady et al. (1994) in which older adults show increased activity in anterior (e.g., frontal) brain regions,

and decreased activity in posterior (e.g., visual) brain regions, and called this the "Posterior-to-Anterior Shift with Ageing" (PASA). Furthermore, it has been hypothesised that one reason for this shift is "functional compensation", whereby older people activate frontal regions to compensate for age-related impairments in posterior brain regions, that is, in order to maintain levels of cognitive performance (Davis et al., 2008; Grady, 2012; Park & Reuter-Lorenz, 2009). However, more recent fMRI studies have questioned whether PASA reflects functional compensation, and suggest instead that the increased frontal activation reflects reduced neural efficiency or specificity (Glisky et al., 2001; Morcom & Henson, 2018; Nyberg et al., 2012; Park et al., 2004; Raz & Rodrigue, 2006; West, 2000). The difference between these two interpretations of the PASA finding is that, whereas the functional compensation hypothesis predicts that anterior increases correlate with better cognitive performance, the inefficiency hypothesis predicts the opposite pattern of anterior increases correlating with worse cognitive performance. This approach can be applied to our current findings, which represent a similar shift from early visual to higher-order regions, albeit during rest rather than during a task. Here too, a compensation account predicts this age-related shift to be associated with better cognitive performance, whereas an inefficiency account predicts the opposite pattern. Our findings support the latter account, i.e., that increased occurrence of higher-order states is associated with worse cognitive performance, specifically in measures of fluid intelligence and particularly in older adults. Importantly, unlike previous reports of the PASA pattern, the current shift was observed during rest, suggesting that it might reflect a stable property of the ageing brain.

The results of our moderation analysis resemble those obtained in a previous study (Tsvetanov et al., 2016), which also investigated the Cam-CAN cohort but using rsfMRI instead, and showed that the relationship between brain connectivity and cognition increased with age. In that case, the authors showed that the cognitive function of older adults becomes increasingly dependent on the balance of excitatory connectivity between networks, and the stability of intrinsic neural representations within networks. Importantly, they used biophysical modelling to account for the confounding effects of vascular health on the fMRI response. However, their results were still limited to static connectivity

driven by the low-frequency fluctuations that are visible to fMRI, and to a small subset of three brain networks (owing to the complexity of the biophysical modelling). The current study overcomes these issues by utilising rsMEG to measure i) the magnetic fields generated by dendritic currents, rather than indirect vascular responses, ii) dynamic connectivity with much higher temporal resolution and iii) whole-brain networks (within the limits of MEG resolution).

Our control analysis, in which we included a quadratic age term to investigate potential non-linear effects of age, yielded an interesting pattern. Namely, unlike the linear age effect, which captures the dissociation between the various network types (e.g., all FTP networks showing similar temporal characteristics, that are distinct from those of the EV networks), the quadratic age effect seems to capture a more general dissociation between the various temporal measures across all networks. Specifically, the quadratic age effect was positive for the number of occurrences across states, but negative for mean life time and mean interval length. Because the linear and quadratic canonical components appear to affect different measures, their combination cannot be simply interpreted in terms of an acceleration/deceleration of the same age effect. We therefore focus here on the simpler, linear effect; the quadratic effect could be explored further in future studies.

One caveat of the current study is that we used cross-sectional data, which precludes direct inferences about ageing (as distinct from cohort effects, owing to year of birth). However, we are not aware of any longitudinal MEG data on such a large, representative population, and until such time, our results can be used to justify and inform hypotheses for future rsMEG studies of ageing. Furthermore, the HMM approach comes with some assumptions. For example, it relies on group concatenation that here assumes anatomical correspondence across the lifespan (though our use of relatively large ROIs minimizes this issue); it requires a priori specification of the number of states, and it uses a Gaussian observation model which may be an oversimplification of the underlying network dynamics (Baker et al., 2014). Another potential limitation of the study is the choice of a relatively coarse parcellation of 38 ROIs for the HMM modelling. This parcellation was used for spatial

dimensionality reduction, in order to make the modelling more tractable and robust to small spatial variations across participants (Quinn et al., 2018). The parcellation used here is the same as that used previously to estimate large-scale functional connectivity networks in MEG (Colclough et al., 2015, 2016; Colclough et al., 2017; Quinn et al., 2018). The use of a relatively coarse parcellation is consistent with evidence that the effective dimensionality in MEG sensor data (following removal of environmental components) is ~70 (Taulu & Simola, 2006); reinforced by findings from adaptive parcellation approaches that find ~70 ROIs is optimal based on the MEG cross-talk function (Farahibozorg et al., 2018). Nonetheless, the fact remains that with MEG, the spatial resolution of the network modelling is limited relative to fMRI. Finally, for some states (FTP3, EV1, and EV2), the degree to which the state was expressed varied with age. Namely, for FTP3 and EV1 the state expression was lower for older compared to younger participants, whereas the opposite was true for SM2. This suggests that, for these states, the results might be partially driven by variations in the spatial rather than temporal expression of the HMM states and should be interpreted cautiously. Nevertheless, despite these limitations, our study offers novel insights on the relationship between the cognitive sequelae of ageing and the underlying patterns of functional brain dynamics, which may be used in the future for mechanistic justification and assessment of interventions to reduce the personal and societal burden of cognitive impairments in old age.

5 Acknowledgments

The Cambridge Centre for Ageing and Neuroscience (Cam-CAN) research was supported by the Biotechnology and Biological Sciences Research Council (BB/H008217/1); R.T is supported by a British Academy Postdoctoral Fellowship (SUAI/028 RG94188); K.A.T is supported by British Academy (PF160048) and the Guarantors of Brain (G101149); R.H is supported by a UK Medical Research Council grant (SUAG/010 RG91365). The funders had no role in study design, data collection and analysis, decision to publish, or preparation of the manuscript. We are grateful to Mark Woolrich for helpful discussion, and to the Cam-CAN respondents and their primary care teams in Cambridge for their

participation in this study. We also thank colleagues at the MRC Cognition and Brain Sciences Unit MEG and MRI facilities for their assistance. The Cam-CAN corporate author consists of the project principal personnel: Lorraine K Tyler, Carol Brayne, Edward T Bullmore, Andrew C Calder, Rhodri Cusack, Tim Dalgleish, John Duncan, Richard N Henson, Fiona E Matthews, William D Marslen-Wilson, James B Rowe, Meredith A Shafto; Research Associates: Karen Campbell, Teresa Cheung, Simon Davis, Linda Geerligs, Rogier Kievit, Anna McCarrey, Abdur Mustafa, Darren Price, David Samu, Jason R Taylor, Matthias Treder, Kamen A Tsvetanov, Janna van Belle, Nitin Williams; Research Assistants: Lauren Bates, Tina Emery, Sharon Erzinc¸lioglu, Andrew Gadie, Sofia Gerbase, Stanimira Georgieva, Claire Hanley, Beth Parkin, David Troy; Research Interviewers: Jodie Allen, Gillian Amery, Liana Amunts, Anne Barcroft, Amanda Castle, Cheryl Dias, Jonathan Dowrick, Melissa Fair, Hayley Fisher, Anna Goulding, Adarsh Grewal, Geoff Hale, Andrew Hilton, Frances Johnson, Patricia Johnston, Thea Kavanagh-Williamson, Magdalena Kwasniewska, Alison McMinn, Kim Norman, Jessica Penrose, Fiona Roby, Diane Rowland, John Sargeant, Maggie Squire, Beth Stevens, Aldabra Stoddart, Cheryl Stone, Tracy Thompson, Ozlem Yazlik; and administrative staff: Dan Barnes, Marie Dixon, Jaya Hillman, Joanne Mitchell, Laura Villis. The authors declare no competing interests.

6 Disclosure Statement

The authors declare no competing interests.

References

Ackerman, P. L., & Rolfhus, E. L. (1999). The locus of adult intelligence: Knowledge, abilities, and nonability traits. *Psychology and Aging*, *14*(2), 314–330. https://doi.org/10.1037/0882-7974.14.2.314

Allen, E. A., Damaraju, E., Plis, S. M., Erhardt, E. B., Eichele, T., & Calhoun, V. D. (2014). Tracking Whole-Brain Connectivity Dynamics in the Resting State. *Cerebral Cortex (New York, NY)*, *24*(3), 663–676. https://doi.org/10.1093/cercor/bhs352

Andrews-Hanna, J. R., Snyder, A. Z., Vincent, J. L., Lustig, C., Head, D., Raichle, M. E., & Buckner, R. L. (2007). Disruption of large-scale brain systems in advanced aging. *Neuron*, *56*(5), 924–935. https://doi.org/10.1016/j.neuron.2007.10.038

Baker, A. P., Brookes, M. J., Rezek, I. A., Smith, S. M., Behrens, T., Probert Smith, P. J., & Woolrich, M. (2014). Fast transient networks in spontaneous human brain activity. *ELife*, *3*, e01867. https://doi.org/10.7554/eLife.01867

Bates, D., Kliegl, R., Vasishth, S., & Baayen, H. (2018). Parsimonious Mixed Models. *ArXiv:1506.04967 [Stat]*. http://arxiv.org/abs/1506.04967

Beard, J. R., Officer, A. M., & Cassels, A. K. (2016). The World Report on Ageing and Health. *The Gerontologist*, *56*(Suppl_2), S163–S166. https://doi.org/10.1093/geront/gnw037

Borgeest, G. S., Henson, R., Shafto, M., Samu, D., Cam-CAN, & Kievit, R. (2018). *Greater lifestyle engagement is associated with better cognitive resilience* [Preprint]. PsyArXiv. https://doi.org/10.31234/osf.io/6pzve

Brookes, M. J., Groom, M. J., Liuzzi, L., Hill, R. M., Smith, H. J. F., Briley, P. M., Hall, E. L., Hunt, B. A. E., Gascoyne, L. E., Taylor, M. J., Liddle, P. F., Morris, P. G., Woolrich, M. W., & Liddle, E. B. (2018). Altered temporal stability in dynamic neural networks underlies connectivity changes in neurodevelopment. *NeuroImage*, *174*, 563–575. https://doi.org/10.1016/j.neuroimage.2018.03.008

Cabral, J., Vidaurre, D., Marques, P., Magalhães, R., Silva Moreira, P., Miguel Soares, J., Deco, G., Sousa, N., & Kringelbach, M. L. (2017). Cognitive performance in healthy older adults relates to spontaneous switching between states of functional connectivity during rest. *Scientific Reports*, *7*(1), 5135. https://doi.org/10.1038/s41598-017-05425-7

Chan, M. Y., Park, D. C., Savalia, N. K., Petersen, S. E., & Wig, G. S. (2014). Decreased segregation of brain systems across the healthy adult lifespan. *Proceedings of the National Academy of Sciences of the United States of America*, *111*(46), E4997-5006. https://doi.org/10.1073/pnas.1415122111

Colclough, G. L., Brookes, M. J., Smith, S. M., & Woolrich, M. W. (2015). A symmetric multivariate leakage correction for MEG connectomes. *NeuroImage*, *117*, 439–448. https://doi.org/10.1016/j.neuroimage.2015.03.071

Colclough, G. L., Woolrich, M. W., Tewarie, P. K., Brookes, M. J., Quinn, A. J., & Smith, S. M. (2016). How reliable are MEG resting-state connectivity metrics? *NeuroImage*, *138*, 284–293. https://doi.org/10.1016/j.neuroimage.2016.05.070

Colclough, G. L, Smith, S. M., Nichols, T. E., Winkler, A. M., Sotiropoulos, S. N., Glasser, M. F., Van Essen, D. C., & Woolrich, M. W. (2017). The heritability of multi-modal connectivity in human brain activity. *ELife*, *6*, e20178. https://doi.org/10.7554/eLife.20178

Davis, S. W., Dennis, N. A., Daselaar, S. M., Fleck, M. S., & Cabeza, R. (2008). Qué PASA? The Posterior–Anterior Shift in Aging. *Cerebral Cortex*, *18*(5), 1201–1209. https://doi.org/10.1093/cercor/bhm155

Drag, L. L., & Bieliauskas, L. A. (2010). Contemporary Review 2009: Cognitive Aging. *Journal of Geriatric Psychiatry and Neurology*, *23*(2), 75–93. https://doi.org/10.1177/0891988709358590

Enders, C. K., & Bandalos, D. L. (2001). The Relative Performance of Full Information Maximum Likelihood Estimation for Missing Data in Structural Equation Models. *Structural Equation*

Modeling: A Multidisciplinary Journal, *8*(3), 430–457. https://doi.org/10.1207/S15328007SEM0803_5

Farahibozorg, S.-R., Henson, R. N., & Hauk, O. (2018). Adaptive cortical parcellations for source reconstructed EEG/MEG connectomes. *NeuroImage*, *169*, 23–45. https://doi.org/10.1016/j.neuroimage.2017.09.009

Ferreira, L. K., & Busatto, G. F. (2013). Resting-state functional connectivity in normal brain aging. *Neuroscience and Biobehavioral Reviews*, *37*(3), 384–400. https://doi.org/10.1016/j.neubiorev.2013.01.017

Folstein, M. F., Folstein, S. E., & McHugh, P. R. (1975). "Mini-mental state". A practical method for grading the cognitive state of patients for the clinician. *Journal of Psychiatric Research*, *12*(3), 189–198. https://doi.org/10.1016/0022-3956(75)90026-6

Geerligs, L., Maurits, N. M., Renken, R. J., & Lorist, M. M. (2014). Reduced specificity of functional connectivity in the aging brain during task performance. *Human Brain Mapping*, *35*(1), 319–330. https://doi.org/10.1002/hbm.22175

Geerligs, L., Renken, R. J., Saliasi, E., Maurits, N. M., & Lorist, M. M. (2015). A Brain-Wide Study of Age-Related Changes in Functional Connectivity. *Cerebral Cortex (New York, N.Y.: 1991)*, *25*(7), 1987–1999. https://doi.org/10.1093/cercor/bhu012

Geerligs, L., Tsvetanov, K. A., Cam-CAN, & Henson, R. N. (2017). Challenges in measuring individual differences in functional connectivity using fMRI: The case of healthy aging. *Human Brain Mapping*, *38*(8), 4125–4156. https://doi.org/10.1002/hbm.23653

Glisky, E. L., Rubin, S. R., & Davidson, P. S. R. (2001). Source memory in older adults: An encoding or retrieval problem? *Journal of Experimental Psychology: Learning, Memory, and Cognition*, *27*(5), 1131–1146. https://doi.org/10.1037/0278-7393.27.5.1131

Gottfredson, L. S., & Deary, I. J. (2004). Intelligence Predicts Health and Longevity, but Why? *Current Directions in Psychological Science*, *13*(1), 1–4. https://doi.org/10.1111/j.0963-7214.2004.01301001.x

Grady, C. (2012). The cognitive neuroscience of ageing. *Nature Reviews Neuroscience*, *13*(7), 491–505. https://doi.org/10.1038/nrn3256

Grady, C. L., Maisog, J. M., Horwitz, B., Ungerleider, L. G., Mentis, M. J., Salerno, J. A., Pietrini, P., Wagner, E., & Haxby, J. V. (1994). Age-related changes in cortical blood flow activation during visual processing of faces and location. *The Journal of Neuroscience: The Official Journal of the Society for Neuroscience*, *14*(3 Pt 2), 1450–1462.

Grady, C. L., Sarraf, S., Saverino, C., & Campbell, K. (2016). Age differences in the functional interactions among the default, frontoparietal control, and dorsal attention networks. *Neurobiology of Aging*, *41*, 159–172. https://doi.org/10.1016/j.neurobiolaging.2016.02.020

Grady, C. L. (2008). Cognitive neuroscience of aging. *Annals of the New York Academy of Sciences*, *1124*, 127–144. https://doi.org/10.1196/annals.1440.009

Hawkins, E., Akarca, D., Zhang, M., Brkić, D., Woolrich, M., Baker, K., & Astle, D. (2020). Functional network dynamics in a neurodevelopmental disorder of known genetic origin. *Human Brain Mapping*, *41*(2), 530–544. https://doi.org/10.1002/hbm.24820

Hedden, T., & Gabrieli, J. D. E. (2004). Insights into the ageing mind: A view from cognitive neuroscience. *Nature Reviews Neuroscience*, *5*(2), 87–96. https://doi.org/10.1038/nrn1323

Hoffmann, H. (2015). *Violin Plot*. Violin Plot Based on Kernel Density Estimation, Using Default Ksdensity. https://uk.mathworks.com/matlabcentral/fileexchange/45134-violin-plot

Horn, J. L., & Cattell, R. B. (1967). Age differences in fluid and crystallized intelligence. *Acta Psychologica*, *26*, 107–129. https://doi.org/10.1016/0001-6918(67)90011-X

Kemper, S., & Sumner, A. (2001). The structure of verbal abilities in young and older adults. *Psychology and Aging*, *16*(2), 312–322. https://doi.org/10.1037/0882-7974.16.2.312

Kovacevic, N., Abdi, H., Beaton, D., & McIntosh, A. R. (2013). Revisiting PLS Resampling: Comparing Significance Versus Reliability Across Range of Simulations. In H. Abdi, W. W. Chin, V. Esposito Vinzi, G. Russolillo, & L. Trinchera (Eds.), *New Perspectives in Partial Least Squares*

and Related Methods (pp. 159–170). Springer. https://doi.org/10.1007/978-1-4614-8283-3_10

Lee, M. H., Smyser, C. D., & Shimony, J. S. (2013). Resting-State fMRI: A Review of Methods and Clinical Applications. *American Journal of Neuroradiology*, *34*(10), 1866–1872. https://doi.org/10.3174/ajnr.A3263

Lehmann, B. C. L., White, S. R., Henson, R. N., Cam-CAN, & Geerligs, L. (2017). Assessing dynamic functional connectivity in heterogeneous samples. *NeuroImage*, *157*, 635–647. https://doi.org/10.1016/j.neuroimage.2017.05.065

Maknojia, S., Churchill, N. W., Schweizer, T. A., & Graham, S. J. (2019). Resting State fMRI: Going Through the Motions. *Frontiers in Neuroscience*, *13*. https://doi.org/10.3389/fnins.2019.00825

McIntosh, A. R., Vakorin, V., Kovacevic, N., Wang, H., Diaconescu, A., & Protzner, A. B. (2014). Spatiotemporal Dependency of Age-Related Changes in Brain Signal Variability. *Cerebral Cortex (New York, NY)*, *24*(7), 1806–1817. https://doi.org/10.1093/cercor/bht030

Morcom, A. M., & Henson, R. N. A. (2018). Increased Prefrontal Activity with Aging Reflects Nonspecific Neural Responses Rather than Compensation. *Journal of Neuroscience*, *38*(33), 7303–7313. https://doi.org/10.1523/JNEUROSCI.1701-17.2018

Nyberg, L., Lövdén, M., Riklund, K., Lindenberger, U., & Bäckman, L. (2012). Memory aging and brain maintenance. *Trends in Cognitive Sciences*, *16*(5), 292–305. https://doi.org/10.1016/j.tics.2012.04.005

Park, D. C., Polk, T. A., Park, R., Minear, M., Savage, A., & Smith, M. R. (2004). Aging reduces neural specialization in ventral visual cortex. *Proceedings of the National Academy of Sciences*, *101*(35), 13091–13095. https://doi.org/10.1073/pnas.0405148101

Park, D. C., & Reuter-Lorenz, P. (2009). The Adaptive Brain: Aging and Neurocognitive Scaffolding. *Annual Review of Psychology*, *60*(1), 173–196. https://doi.org/10.1146/annurev.psych.59.103006.093656

Petrican, R., & Grady, C. L. (2017). Contextual and Developmental Differences in the Neural Architecture of Cognitive Control. *Journal of Neuroscience*, *37*(32), 7711–7726. https://doi.org/10.1523/JNEUROSCI.0667-17.2017

Petrican, R., & Grady, C. L. (2019). The intrinsic neural architecture of inhibitory control: The role of development and emotional experience. *Neuropsychologia*, *127*, 93–105. https://doi.org/10.1016/j.neuropsychologia.2019.01.021

Power, J. D., Barnes, K. A., Snyder, A. Z., Schlaggar, B. L., & Petersen, S. E. (2012). Spurious but systematic correlations in functional connectivity MRI networks arise from subject motion. *NeuroImage*, *59*(3), 2142–2154. https://doi.org/10.1016/j.neuroimage.2011.10.018

Quinn, A. J., Vidaurre, D., Abeysuriya, R., Becker, R., Nobre, A. C., & Woolrich, M. W. (2018). Task-Evoked Dynamic Network Analysis Through Hidden Markov Modeling. *Frontiers in Neuroscience*, *12*. https://doi.org/10.3389/fnins.2018.00603

Raz, N., & Rodrigue, K. M. (2006). Differential aging of the brain: Patterns, cognitive correlates and modifiers. *Neuroscience & Biobehavioral Reviews*, *30*(6), 730–748. https://doi.org/10.1016/j.neubiorev.2006.07.001

Rezek, I., & Roberts, S. (2005). Ensemble Hidden Markov Models with Extended Observation Densities for Biosignal Analysis. In D. Husmeier, R. Dybowski, & S. Roberts (Eds.), *Probabilistic Modeling in Bioinformatics and Medical Informatics* (pp. 419–450). Springer. https://doi.org/10.1007/1-84628-119-9_14

Rosner, B. (1983). Percentage Points for a Generalized ESD Many-Outlier Procedure. *Technometrics*, *25*(2), 165–172. https://doi.org/10.1080/00401706.1983.10487848

Rosseel, Y. (2012). Lavaan: An R package for structural equation modeling. *JOURNAL OF STATISTICAL SOFTWARE*, *48*(2), 1–36.

Schaie, K. W. (1994). The course of adult intellectual development. *American Psychologist*, *49*(4), 304–313. https://doi.org/10.1037/0003-066X.49.4.304

Shafto, M. A., Tyler, L. K., Dixon, M., Taylor, J. R., Rowe, J. B., Cusack, R., Calder, A. J., Marslen-Wilson, W. D., Duncan, J., Dalgleish, T., Henson, R. N., Brayne, C., Matthews, F. E., & Cam-CAN. (2014). The Cambridge Centre for Ageing and Neuroscience (Cam-CAN) study protocol: A cross-sectional, lifespan, multidisciplinary examination of healthy cognitive ageing. *BMC Neurology*, *14*(1), 204. https://doi.org/10.1186/s12883-014-0204-1

Sherry, A., & Henson, R. K. (2005). Conducting and Interpreting Canonical Correlation Analysis in Personality Research: A User-Friendly Primer. *Journal of Personality Assessment*, *84*(1), 37–48. https://doi.org/10.1207/s15327752jpa8401_09

Singer, T., Verhaeghen, P., Ghisletta, P., Lindenberger, U., & Baltes, P. B. (2003). The fate of cognition in very old age: Six-year longitudinal findings in the Berlin Aging Study (BASE). *Psychology and Aging*, *18*(2), 318–331. https://doi.org/10.1037/0882-7974.18.2.318

Skinner, H. A. (1982). The Drug Abuse Screening Test. *Addictive Behaviors*, *7*(4), 363–371. https://doi.org/10.1016/0306-4603(82)90005-3

Smith, S. M., Nichols, T. E., Vidaurre, D., Winkler, A. M., Behrens, T. E. J., Glasser, M. F., Ugurbil, K., Barch, D. M., Van Essen, D. C., & Miller, K. L. (2015). A positive-negative mode of population covariation links brain connectivity, demographics and behavior. *Nature Neuroscience*, *18*(11), 1565–1567. https://doi.org/10.1038/nn.4125

Snellen, H. (1862). *Letterproeven, tot bepaling der gezigtsscherpte*. J. Greven.

Sui, J., Adali, T., Yu, Q., Chen, J., & Calhoun, V. D. (2012). A review of multivariate methods for multimodal fusion of brain imaging data. *Journal of Neuroscience Methods*, *204*(1), 68–81. https://doi.org/10.1016/j.jneumeth.2011.10.031

Taulu, S., & Simola, J. (2006). Spatiotemporal signal space separation method for rejecting nearby interference in MEG measurements. *Physics in Medicine and Biology*, *51*(7), 1759–1768. https://doi.org/10.1088/0031-9155/51/7/008

Taylor, J. R., Williams, N., Cusack, R., Auer, T., Shafto, M. A., Dixon, M., Tyler, L. K., Cam-CAN, & Henson, R. N. (2017). The Cambridge Centre for Ageing and Neuroscience (Cam-CAN) data

repository: Structural and functional MRI, MEG, and cognitive data from a cross-sectional adult lifespan sample. *NeuroImage*, *144*, 262–269. https://doi.org/10.1016/j.neuroimage.2015.09.018

Tsvetanov, K. A., Henson, R. N. A., & Rowe, J. B. (2019). Separating vascular and neuronal effects of age on fMRI BOLD signals. *ArXiv:1912.02899 [q-Bio]*. http://arxiv.org/abs/1912.02899

Tsvetanov, K. A., Henson, R. N. A., Tyler, L. K., Davis, S. W., Shafto, M. A., Taylor, J. R., Williams, N., Cam-CAN, & Rowe, J. B. (2015). The effect of ageing on fMRI: Correction for the confounding effects of vascular reactivity evaluated by joint fMRI and MEG in 335 adults. *Human Brain Mapping*, *36*(6), 2248–2269. https://doi.org/10.1002/hbm.22768

Tsvetanov, K. A., Henson, R. N. A., Tyler, L. K., Razi, A., Geerligs, L., Ham, T. E., Rowe, J. B., & Neuroscience, C. C. for A. and. (2016). Extrinsic and Intrinsic Brain Network Connectivity Maintains Cognition across the Lifespan Despite Accelerated Decay of Regional Brain Activation. *Journal of Neuroscience*, *36*(11), 3115–3126. https://doi.org/10.1523/JNEUROSCI.2733-15.2016

Tsvetanov, K. A., Ye, Z., Hughes, L., Samu, D., Treder, M. S., Wolpe, N., Tyler, L. K., Rowe, J. B., & Neuroscience, for the C. C. for A. and. (2018). Activity and Connectivity Differences Underlying Inhibitory Control Across the Adult Life Span. *Journal of Neuroscience*, *38*(36), 7887–7900. https://doi.org/10.1523/JNEUROSCI.2919-17.2018

Tucker-Drob, E. M. (2011). Neurocognitive functions and everyday functions change together in old age. *Neuropsychology*, *25*(3), 368–377. https://doi.org/10.1037/a0022348

Uttl, B. (2002). North American Adult Reading Test: Age norms, reliability, and validity. *Journal of Clinical and Experimental Neuropsychology*, *24*(8), 1123–1137. https://doi.org/10.1076/jcen.24.8.1123.8375

Van Veen, B. D., Van Drongelen, W., Yuchtman, M., & Suzuki, A. (1997). Localization of brain electrical activity via linearly constrained minimum variance spatial filtering. *IEEE Transactions on Biomedical Engineering*, *44*(9), 867–880. https://doi.org/10.1109/10.623056

Verhaeghen, P. (2003). Aging and vocabulary score: A meta-analysis. *Psychology and Aging*, *18*(2), 332–339. https://doi.org/10.1037/0882-7974.18.2.332

Vidaurre, D., Abeysuriya, R., Becker, R., Quinn, A. J., Alfaro-Almagro, F., Smith, S. M., & Woolrich, M. W. (2018). Discovering dynamic brain networks from big data in rest and task. *NeuroImage*, *180*, 646–656. https://doi.org/10.1016/j.neuroimage.2017.06.077

Vidaurre, D., Quinn, A. J., Baker, A. P., Dupret, D., Tejero-Cantero, A., & Woolrich, M. W. (2016). Spectrally resolved fast transient brain states in electrophysiological data. *NeuroImage*, *126*, 81–95. https://doi.org/10.1016/j.neuroimage.2015.11.047

Vidaurre, D., Smith, S. M., & Woolrich, M. W. (2017). Brain network dynamics are hierarchically organized in time. *Proceedings of the National Academy of Sciences of the United States of America*, *114*(48), 12827–12832. https://doi.org/10.1073/pnas.1705120114

Wang, H.-T., Smallwood, J., Mourao-Miranda, J., Xia, C. H., Satterthwaite, T. D., Bassett, D. S., & Bzdok, D. (2020). Finding the needle in a high-dimensional haystack: Canonical correlation analysis for neuroscientists. *NeuroImage*, *216*, 116745. https://doi.org/10.1016/j.neuroimage.2020.116745

West, R. (2000). In defense of the frontal lobe hypothesis of cognitive aging. *Journal of the International Neuropsychological Society*, *6*(6), 727–729. https://doi.org/10.1017/S1355617700666109

Woolrich, M., Hunt, L., Groves, A., & Barnes, G. (2011). MEG beamforming using Bayesian PCA for adaptive data covariance matrix regularization. *NeuroImage*, *57*(4), 1466–1479. https://doi.org/10.1016/j.neuroimage.2011.04.041

Supplementary Materials

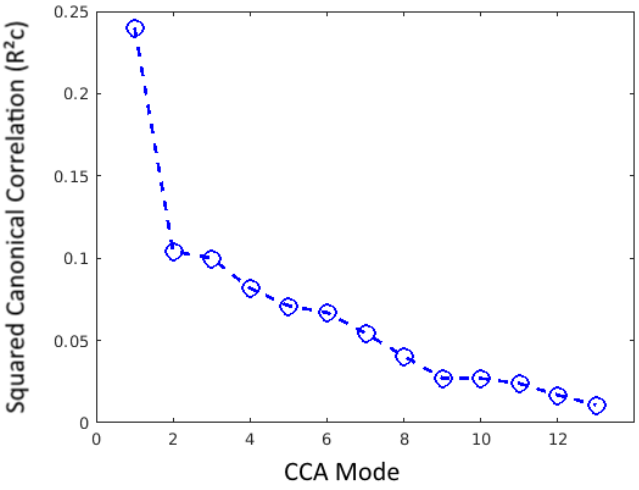

Supplementary Figure 1. Squared canonical correlation (R^2c) for each CCA mode in the Cognition ~ HMM profile CCA, which represents the proportion of variance shared by the two synthetic variates. Only the first CCA mode, which accounted for a substantial portion of the shared variance (R^2c = 24%), was interpreted.

Supplementary Tables 1 and 2 include the standardized canonical coefficients (*Coef*), the structure coefficients (r_s) and the squares structure coefficients (r^2_s) for the canonical solutions. Note that in both tables, the difference between the function and the structure coefficients, together with function coefficients that are greater than 1 or lower than -1, indicate multicollinearity in our CCA model. Therefore, as mentioned in the main text, we used structure coefficients to guide our interpretation.

Supplementary Table 1. Canonical solution for the CCA relating HMM measures with age

	Measure	State	*Coef*	r_s	r^2_s *(%)*
Set A	Fractional Occupancy	FTP1	2.13	.27	7.46
		FTP2	0.73	.23	5.43
		FTP3	-1.38	.20	3.9
		HOV	-1.39	.23	5.38
		EV1	0	-.35	11.97
		EV2	0.81	-.45	20.35
		SM1	1.03	.18	3.19
		SM2	3.14	-.03	0.12
	Mean Lifetime	FTP1	-0.33	.13	1.75
		FTP2	-0.04	.15	2.21
		FTP3	1.03	.44	19.77
		HOV	1.28	.15	2.33
		EV1	0.3	-.50	26.18
		EV2	0.04	-.38	14.52
		SM1	-0.35	.04	0.14
		SM2	-0.94	-.09	0.73
	Number of Occurrences	FTP1	-1.56	.28	7.61
		FTP2	-0.34	.24	5.74
		FTP3	2.1	.12	1.43
		HOV	2.25	.34	11.68
		EV1	-0.06	-.00	0
		EV2	-0.52	-.33	10.72
		SM1	0.17	.22	5.05
		SM2	-1.89	.00	0
	Mean Interval Length	FTP1	0.16	-.12	1.46
		FTP2	-0.06	-.21	4.34
		FTP3	0.35	-.07	0.5
		HOV	0.06	-.07	0.63
		EV1	-0.59	-.01	0.02
		EV2	-0.3	.18	3.26
		SM1	0.02	-.13	1.67
		SM2	0.13	.02	0.02
Set B	Age		1	1	1

Note. The various states are indicated as *FTP* (frontotemporoparietal), *HOV* (higher-order visual), *EV* (early-visual) and *SM* (sensorimotor). *Coef* = standardized canonical function coefficient; r_s = structure coefficient; r^2_s = squared structure coefficient.

Supplementary Table 2. Canonical solution for the CCA relating HMM measures with cognitive measures

	Measure	State	*Coef*	r_s	r^2_s (%)
Set A	Fractional Occupancy	FTP1	2.03	.29	8.46
		FTP2	0.99	.25	6.08
		FTP3	-0.86	.37	13.56
		HOV	-0.9	.19	3.52
		EV1	0	-.35	11.96
		EV2	0.69	-.43	18.7
		SM1	0.78	.15	2.34
		SM2	3.08	-.07	0.5
	Mean Lifetime	FTP1	-0.26	.15	2.17
		FTP2	-0.2	.06	0.36
		FTP3	0.94	.53	28.42
		HOV	0.99	.12	1.54
		EV1	0.56	-.49	24
		EV2	-0.11	-.41	16.76
		SM1	-0.19	0	0
		SM2	-0.98	-.15	2.39
	Number of Occurrences	FTP1	-1.46	.29	8.34
		FTP2	-0.35	.27	7.32
		FTP3	2.05	.28	8.06
		HOV	1.91	.26	6.53
		EV1	0.09	-.02	0.05
		EV2	-0.21	-.28	7.92
		SM1	0.09	.21	4.57
		SM2	-1.62	-.01	0
	Mean Interval Length	FTP1	-0.01	-.10	0.9
		FTP2	-0.02	-.16	2.52
		FTP3	0.67	-.16	2.67
		HOV	0.13	-.02	0.04
		EV1	-0.4	.03	0.12
		EV2	-0.07	.19	3.76
		SM1	-0.29	-.14	1.87
		SM2	0.33	.04	0.16
Set B	Fluid Intelligence	FldIn	-0.12	-.73	52.84
		FacRec	0.09	-.38	14.82
		EmoRec	-0.02	-.48	23.39
		MltTs	0.09	.34	11.73
		PicNam	-0.57	-.82	67.47
		MRSp	0.1	.46	21.41
		MRCv	-0.39	-.75	56.1
		VSTM	-0.14	-.61	36.94
		StrRec	0.08	-.41	16.64
		VrbFl	0.02	-.41	16.85
	Crystallized Intelligence	SntRec	-0.05	-.32	10.37
		ProV	0.06	.06	0.41
		StW	0.23	.15	2.15

Note. Cognitive measures are fluid intelligence (*FldIn*), face recognition (*FacRec*), emotional expression recognition (*EmoRec*), multitasking (hotel task; *MltTs*), picture-picture priming (*PicNam*), choice motor speed (*MRSp*), choice motor coefficient of variation (*MRCv*), visual short-term memory (*VSTM*), story recall (*StrRec*), verbal fluency (*VrbFl*), sentence comprehension (*SntRec*), proverb comprehension (*ProV*), and spot the word (*StW*). The various states are indicated as *FTP* (frontotemporoparietal), *HOV* (higher-order visual), *EV* (early-visual) and *SM* (sensorimotor). *Coef* = standardized canonical function coefficient; r_s = structure coefficient; r^2_s = squared structure coefficient.

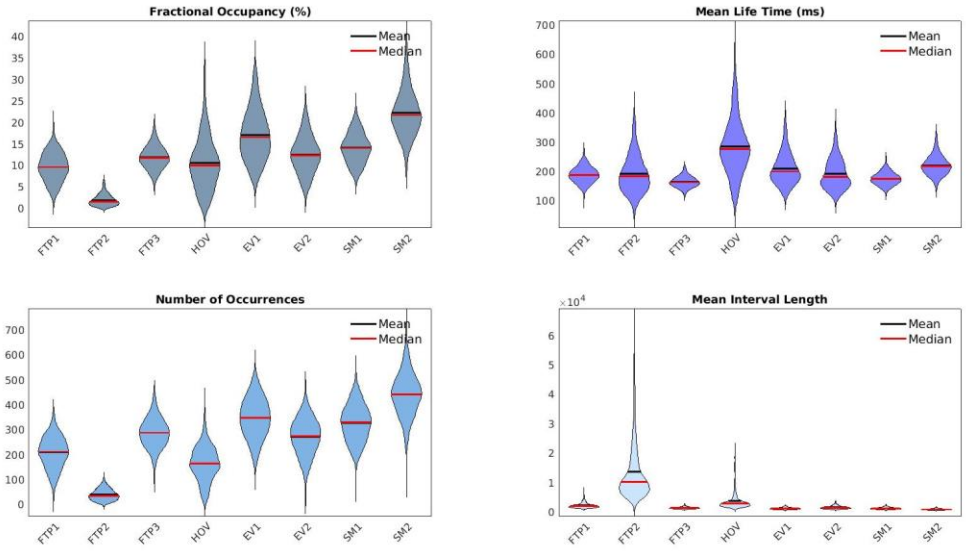

Supplementary Figure 2. Violin plots (Hoffmann, 2015) of the four temporal characteristics of the HMM states, following the removal of outliers (SD > 3 in any of the measures): % fractional occupancy (FO; top-left), mean life time (MLT; top right), number of occurrences (NO; bottom-left) mean interval length (MIL; bottom-right) following the removal of outliers (*SD* > 3 in one or more HMM measures). The various states are indicated as *FTP* (frontotemporoparietal), *HOV* (higher-order visual), *EV* (early-visual) and *SM* (sensorimotor). The first three measures are positive measures (i.e., indicate more frequent/longer duration of state's occurrence), whereas the fourth measure (MIL) is a negative measure. Mean and median are indicated by black and red lines, respectively (N=496).

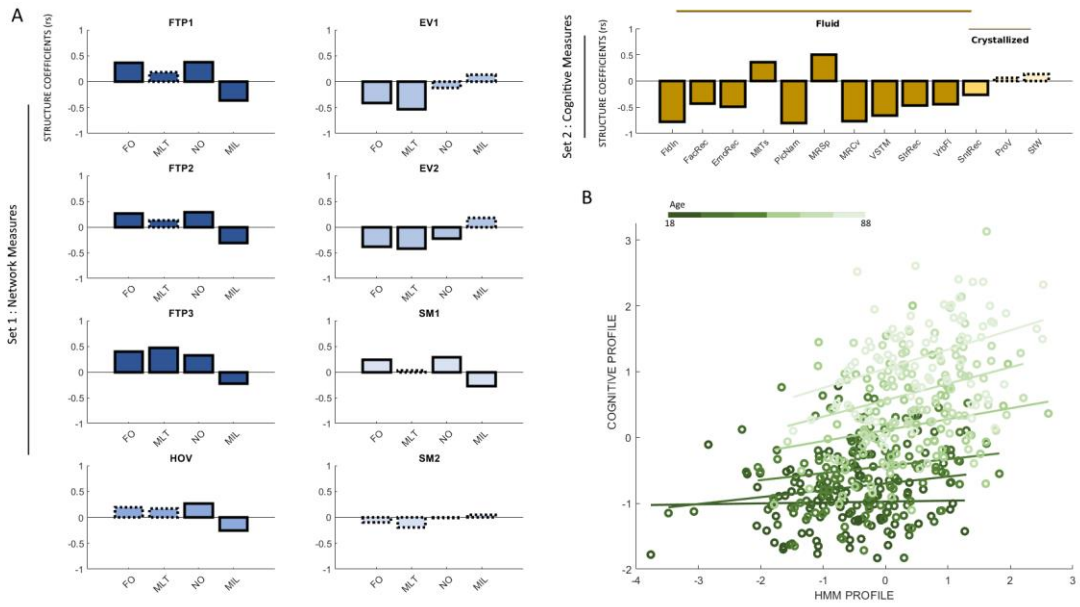

Supplementary Figure 3. Outcomes of CCA and moderation analyses with n=496, following the removal of outliers (*SD* > 3 in one or more HMM measures).

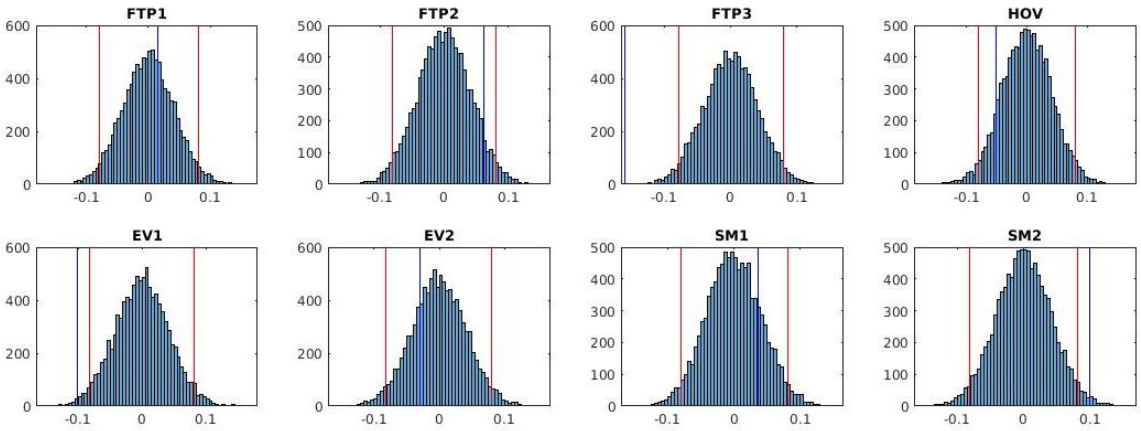

Supplementary Figure 4. HMM expression of each state across age. Blue lines indicate Pearson correlation coefficient (*R*) for the relation between the HMM fit (calculated as the correlation between group-based partial correlations and the partial correlation of each participant) and age. Red lines indicate *R* at 2.5% and at 97.5% of the distribution of permutation data represented by the histogram (equivalent to p = .05). The various states are indicated as *FTP* (frontotemporoparietal), *HOV* (higher-order visual), *EV* (early-visual) and *SM* (sensorimotor). The spatial profiles of states FTP3 and EV1 reliably decreased with age, while that for SM2 reliably increased with age.

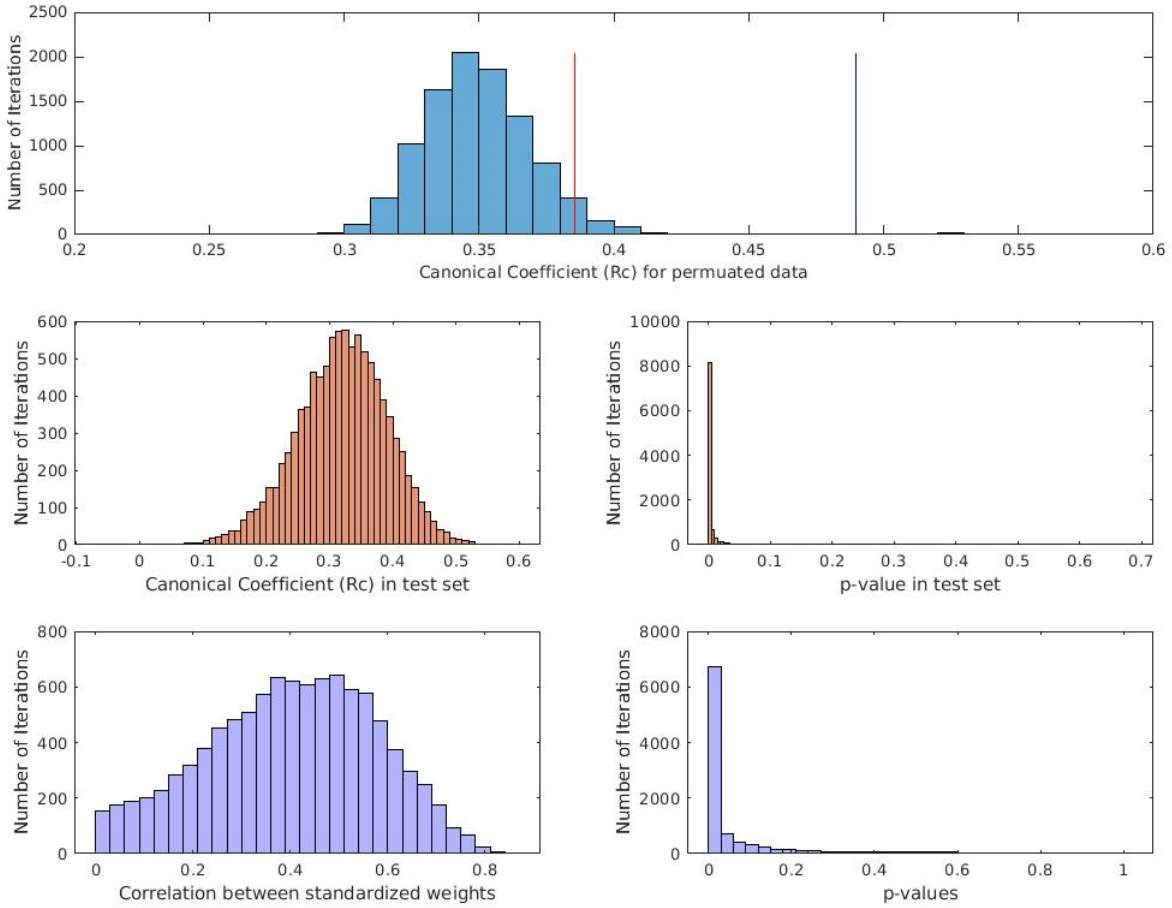

Supplementary Figure 5. Outcomes of control analyses. Top: histogram of canonical coefficients (R_c) of the first CCA mode for permutated data across 10,000 iterations. Red line indicates R_c at 95% of the distribution of permutation data (equivalent to p = .05). Blue line indicates R_c obtained with the actual data. Middle: histogram of Rc (left) and p-values (right) of the first CCA mode in the test set after applying weight vectors from the train set, across 10,000 iterations. Bottom: outcomes of the analysis comparing standardized canonical function coefficients across subsets of the data: distribution of Spearman coefficients across 10,000 iterations, each with different partitioning of the data (left) and distribution of p-values of these correlations (right).

Supplementary Analysis 1

Below are the effects of age on the probability of transitions between the various brain states. For each participant, a transition probability matrix was computed, reflecting the probability to transition between every pair of states. The mean transition probabilities are shown Panel A of Supplementary Figure 6 below, after excluding the diagonal (which does not represent a transition, and is therefore always zero), and excluding unlikely transitions (i.e., those that occurred for less than 50% of the participants). The remaining 35 transitions were vectorised, z-scored, and subjected to CCA in order to relate them with age. Structure coefficients associated with this analysis are shown in Panel B of Supplementary Figure 6. We do not offer an interpretation of these results, but include them for completeness.

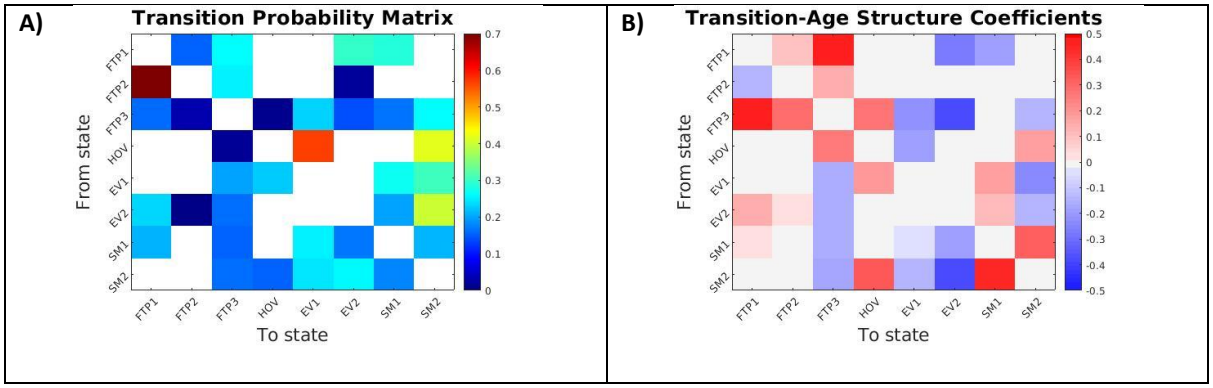

Supplementary Figure 6. Transition probabilities and their relations to age. The various states are indicated as *FTP* (frontotemporoparietal), *HOV* (higher-order visual), *EV* (early-visual) and *SM* (sensorimotor). **(A)** Transition probability matrix, averaged across participants, reflecting the probability to transition between every pair of states, after excluding the diagonal (which does not represent a transition, and is therefore always zero) as well as unlikely transitions (i.e., those that occurred for less than 50% of the participants). **(B)** Structure coefficients (r_s) for the CCA relating transitions to age. Red indicates increased probability of the transition with older age, whereas blue represents decreased probability with older age.